

# $A_0$ : An Affordance-Aware Hierarchical Model for General Robotic Manipulation

Rongtao Xu<sup>1\*</sup>, Jian Zhang<sup>1\*</sup>, Minghao Guo<sup>1\*</sup>, Youpeng Wen<sup>2\*</sup>,  
Haoting Yang<sup>3</sup>, Min Lin<sup>2</sup>, Jianzheng Huang<sup>3</sup>, Zhe Li<sup>3</sup>, Kaidong Zhang<sup>2</sup>, Liqiong Wang<sup>3</sup>,  
Yuxuan Kuang<sup>1</sup>, Meng Cao<sup>1</sup>, Feng Zheng<sup>3†</sup>, Xiaodan Liang<sup>1,2†</sup>

<sup>1</sup>MBZUAI <sup>2</sup>Sun Yat-sen University <sup>3</sup>Southern University of Science and Technology

<https://a-embodied.github.io/A0/>

## Abstract

Robotic manipulation faces critical challenges in understanding spatial affordances—the “where” and “how” of object interactions—essential for complex manipulation tasks like wiping a board or stacking objects. Existing methods, including modular-based and end-to-end approaches, often lack robust spatial reasoning capabilities. Unlike recent point-based and flow-based affordance methods that focus on dense spatial representations or trajectory modeling, we propose  $A_0$ , a hierarchical affordance-aware diffusion model that decomposes manipulation task into high-level spatial affordance understanding and low-level action execution.  $A_0$  leverages the Embodiment-Agnostic Affordance Representation, which captures object-centric spatial affordances by predicting contact point and post-contact trajectories.  $A_0$  is pre-trained on 1 million contact points data and fine-tuned on annotated trajectories, enabling generalization across platforms. Key components include Position Offset Attention for motion-aware feature extraction and a Spatial Information Aggregation Layer for precise coordinate mapping. The model’s output is executed by the action execution module. Experiments on multiple robotic systems (Franka, Kinova, Realman and Dobot) demonstrate  $A_0$ ’s superior performance in complex tasks, showcasing its efficiency, flexibility, and real-world applicability.

## 1. Introduction

Robotic manipulation is a fundamental yet challenging task in robotics and embodied AI, requiring robots to interact with objects in complex environments. Recent advancements focus on two approaches: (1) modular-based methods [20, 25, 29] that use large vision foundation models for spatial understanding, and (2) end-to-end Vision-Language-



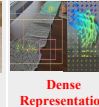


	End-to-end VLA ( $\pi_0$ , RDT)	Modular-based (MOKA, ReKep)	Affordance-based (RoboPoint, Magma)	Hierarchical (Helix)	$A_0$ (Ours)
Learning spatial affordances	✗	✗	✓	✗	✓
Object-centric	✗	✗	✗	✗	✓
Output	 Action Space	 Heatmap/ Waypoints	 Dense Representation	 Action Space	 Object-centric point and Post-contact Trajectories

Figure 1. Comparison of different manipulation methods.  $A_0$  is an object-centric hierarchical model that learns Embodiment-Agnostic Affordance Representation.

Action (VLA) methods [6, 7, 23, 31] for fine-grained manipulation. However, existing methods still face significant limitations in understanding spatial affordances—the “where” and “how” of object interactions—which are critical for achieving spatial intelligence. For example, in tasks like wiping a whiteboard, insufficient understanding of spatial affordances often leads to incomplete or inefficient execution.

Spatial affordances can be learned not only from real-world and synthetic robotic datasets [44] but also from a wide range of out-of-domain data rich in actionable knowledge, such as Internet data [12], and hand-object interaction (HOI) data [57]. These datasets contain valuable information about object interactions, spatial properties, and physical attributes, making it essential to represent actionable knowledge as unified spatial affordances. Modular-based methods, such as ReKep [20] and MOKA [29], directly utilize Large Vision Models (LVM) but lack a deep understanding of the spatial and physical world, particularly in capturing the operability of objects. On the other hand, end-to-end methods like RDT [31] and  $\pi_0$  [6] generate actions directly without adequately understanding spatial positions, leading to suboptimal performance in complex manipulation tasks, such as wiping a board or stacking objects.

\*Equal contribution

†Corresponding authors

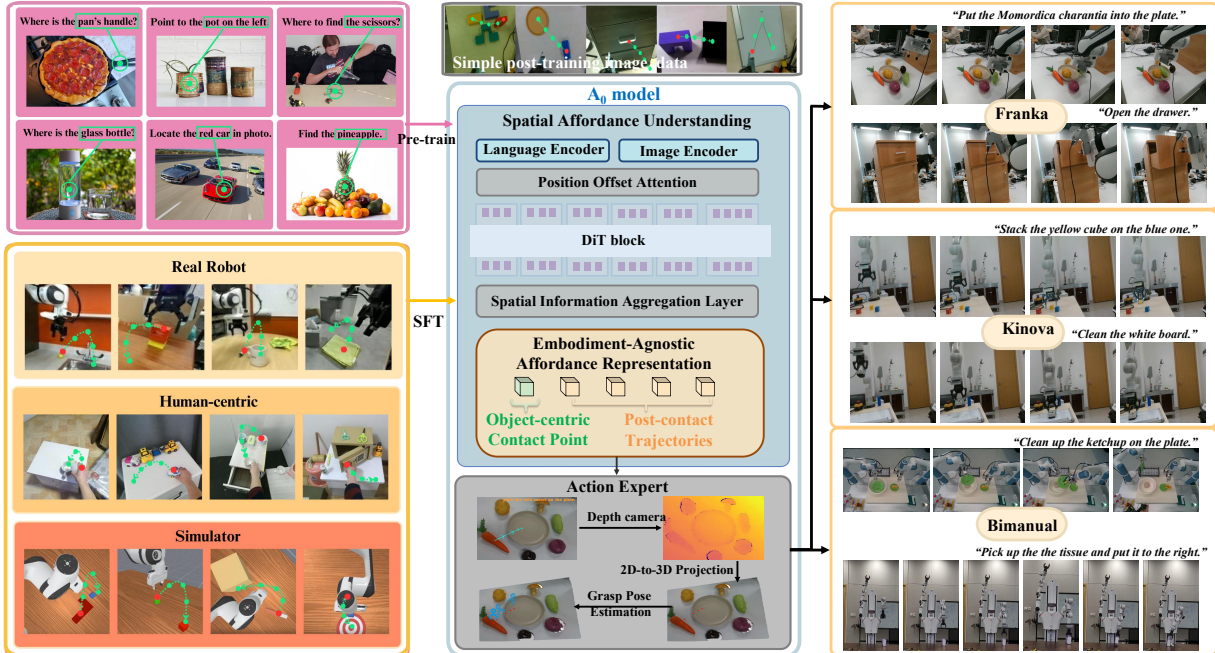


Figure 2. The  $A_0$  model decomposes robotic manipulation tasks into two levels: (1) high-level spatial affordance understanding and (2) low-level action execution.  $A_0$  leverages an Embodiment-Agnostic Affordance Representation to predict object-centric contact points and post-contact trajectories. The architecture includes well-designed key components for affordance learning.  $A_0$  is pre-trained on a large-scale dataset of contact points and fine-tuned on annotated trajectories, enabling generalization across diverse robotic platforms. Zoom-in for the best of views.

Recently, several methods have emerged, recognizing the importance of spatial affordance in robotic manipulation. Point-based methods such as SpatialVLA [41], Any-point Trajectory Modeling [49], RoboPoint [58], Track2Act [5], and flow-based methods such as General Flow [57] and Im2Flow2Act [53] have made significant strides in modeling spatial interactions. However, these methods often focus on dense spatial representations or trajectory modeling (see Figure 1), which can be computationally expensive and embodiment-specific. In contrast, our approach is **object-centric**, focusing solely on predicting the contact point and trajectories of the objects that need to be manipulated. We propose an **Embodiment-Agnostic Affordance Representation** to capture the “where” and “how” of object interactions. This design makes our method **embodiment-agnostic**, enabling seamless generalization across different robotic platforms. By leveraging this general Embodiment-Agnostic Affordance Representation, our approach requires only a small amount of task-specific annotated data for fine-tuning, making it highly practical and general for real-world deployment.

To address the challenge of spatial understanding and physical reasoning in manipulation, we propose  $A_0$ , a novel Affordance-Aware Hierarchical Model specifically designed for robotic manipulation. The model decomposes manipulation tasks into two levels: (1) a high-level **spatial**

**affordance understanding** and (2) a low-level **action execution**. Our model and system architecture are depicted in Figure 2.  $A_0$  primarily focuses on high-level spatial affordance understanding, including object contact points and post-contact trajectories, to guide low-level action execution effectively. To learn foundational localization capabilities,  $A_0$  is pre-trained on 1 million contact-point localization data points, followed by supervised fine-tuning on an annotated spatial trajectory dataset. This hierarchical design enables  $A_0$  to handle complex manipulation tasks more effectively, particularly those requiring spatial affordance reasoning and physical interaction. Our method achieves an average success rate of 62.50% on Franka and 53.75% on Kinova, outperforming the strongest baselines on both platforms. Notably, it demonstrates robust performance in trajectory-following tasks like Wipe Board (45%).

The key contributions of our work are as follows:

- We introduce an **Embodiment-Agnostic Affordance Representation** that efficiently captures spatial affordance by predicting object-centric contact point and trajectories. This representation is supported by a 1 million annotated dataset and an efficient annotation pipeline. The point-based nature of our representation makes it highly versatile and easy to deploy across different robotic platforms.
- We propose a **hierarchical affordance-aware diffusion**

**model**  $A_0$  that first learns Embodiment-Agnostic Affordance Representation and then generates precise manipulation actions. The model incorporates several key components, including Position Offset Attention, DiT blocks, and a Spatial Information Aggregation Layer, to enhance spatial affordance understanding.

- We validate the effectiveness of  $A_0$  on **multiple robotic platforms** (e.g., Franka, Kinova, Realman and Dobot). The model demonstrates superior performance in complex tasks requiring spatial affordance reasoning, such as wiping a whiteboard or placing objects, showcasing its strong generalization capabilities and embodiment-agnostic design.

## 2. Related Works

### 2.1. Spatial Affordance in Robotic Manipulation.

Affordance prediction is crucial for robotic manipulation, enabling structured action selection in complex environments. Current methods vary in input processing: point cloud-based approaches [15, 27, 28, 36, 48, 52] excel in spatial reasoning, while RGB image-based techniques [3, 10, 17–19, 30, 39] prioritize accessibility. Language integration, as in LASO [27] and Chen *et al.* [10], further enhances these methods.

Output representations differ in three ways: 1) *Heatmap-based* methods [3, 10, 15, 27, 28, 36, 39, 48, 52] localize affordances but are computationally intensive; 2) *Bounding box* approaches [17, 18, 30] balance efficiency and accuracy; 3) *Keypoint-based* techniques [19, 30] provide robust representations for articulated objects. Recent advances like MOKA [30] and A3VLM [17] refine keypoint and bounding box methods. Our work improves keypoint-based reasoning by predicting contact points and trajectories, offering precise, efficient action specifications for robotic applications.

### 2.2. VLA and Hierarchical Models

Recent advancements in Vision-Language-Action (VLA) models have enhanced robotic manipulation through multi-modal learning, categorized into transformer-based, VLM-based, and diffusion-based approaches. Transformer-based methods [4, 9, 51] predict action sequences using video generation models. VLM-based approaches [2, 8, 11, 23, 26, 40, 60] leverage pre-trained vision-language models for improved generalization. Diffusion-based frameworks [16, 32, 37, 43, 46, 50] enable probabilistic action generation for robust trajectory planning. GR-2 [9] and OpenVLA [23] exemplify transformer-based and VLM-based methods, respectively, while RDT-1B [32] showcases diffusion-based bimanual manipulation. These models leverage large datasets to enhance real-world robotic applications.

Hierarchical models enhance manipulation capabilities

by organizing control into multiple abstraction levels, enabling robots to generalize across diverse tasks. Dex-GraspNet [47] provides a large-scale dataset and learning framework for hierarchical dexterous grasping, combining high-level planning with low-level control to achieve robust grasps across various object categories. Similarly, Helix [14] adopts a hierarchical reinforcement learning paradigm, leveraging high-level policies to guide low-level motor control, improving both adaptability and efficiency in real-world manipulation scenarios. In the HAMSTER [61] framework, the VILA-1.5-13b VLM is trained to generate textual representations of paths, whereas our method employs DiT to predict the object-centric waypoints.

Unlike VLA methods, which often struggle with embodiment-specific constraints,  $A_0$  leverages a diffusion-based framework for flexible and robust trajectory planning under uncertainty. Compared to hierarchical models,  $A_0$  adopts a hierarchical affordance-aware design that decomposes tasks into high-level spatial affordance understanding and low-level action execution, enabling generalization across diverse tasks and platforms. In contrast, Helix leverages vision-language models (VLMs) to learn latent semantic representations rather than explicit object-centric spatial affordances. By focusing on object-centric spatial affordances,  $A_0$  reduces computational overhead and improves adaptability, making it highly practical for real-world deployment.

## 3. The $A_0$ Model

### 3.1. Overview

We propose the  $A_0$  model to address spatial affordance understanding (the "where" and "how" of object manipulation). As shown in Figure 3,  $A_0$  uses an Embodiment-Agnostic Affordance Representation (See Sec. 3.2) to predict object contact points and trajectories, supported by a multi-dataset annotation pipeline. The model operates hierarchically: (1) high-level spatial affordance understanding and (2) low-level action execution. For spatial understanding, we leverage Diffusion architecture for object affordance learning (See Sec. 3.3). Furthermore, the training strategy includes pre-training on 100,000 contact-point samples and fine-tuning on annotated trajectories (see Sec. 3.4). For action execution, we adopt point-based methods similar to [25, 29] (see Sec. 4).

### 3.2. Embodiment-Agnostic Affordance Representation

To enable the model to effectively understand spatial affordances and capture the "where" and "how" of object interactions, we propose a unified **Embodiment-Agnostic Affordance Representation**  $\mathcal{R}$  that can be easily acquired from diverse data sources. Specifically, this representa-

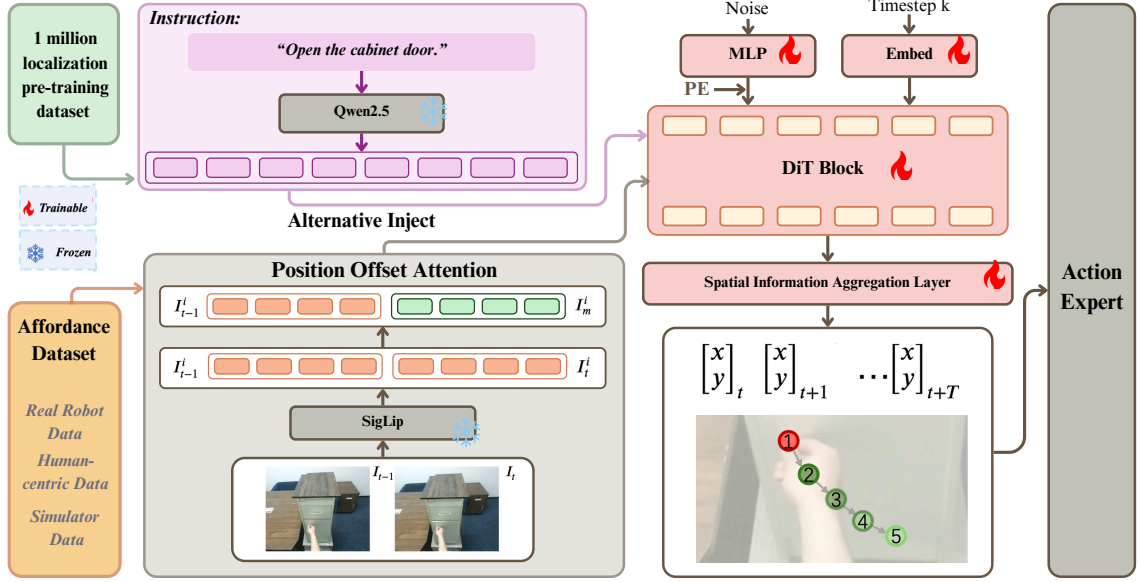


Figure 3. Overview of  $A_0$  model. The model is transformer based diffusion probabilistic model to predict the waypoints for robotic manipulation. We use the pre-trained Qwen2.5-7B [54] and SigLip (400M) [59] to encode the language instruction and images, separately. The image of previous time step are used to provide motion information by the proposed motion token enhancement. The image and text tokens are alternatively injected as conditions via cross attention.

tion integrates actionable knowledge from real-world or synthetic robotic data  $\mathcal{R}_R$ , hand-object interaction (HOI) data  $\mathcal{R}_H$ , and custom data  $\mathcal{R}_C$ . To unify affordance information from these varied sources, each entry in the Embodiment-Agnostic Affordance Representation includes an object-centric RGB image  $I$  (the current frame), a set of 2D waypoints indicating the contact point  $c_0^{2D}$  and post-contact trajectories  $T = (t_0^{2D}, t_1^{2D}, t_2^{2D}, \dots)$ , along with a manipulation task instruction expressed in natural language. Therefore, the constructed Embodiment-Agnostic Affordance Representation can be expressed as:

$$\begin{aligned} \mathcal{R} &= \mathcal{R}_R \cup \mathcal{R}_H \cup \mathcal{R}_C \\ &= \{(I, L, C, T) \mid C = (c_0^{2D}), T = (t_0^{2D}, t_1^{2D}, t_2^{2D}, \dots)\}. \end{aligned} \quad (1)$$

By leveraging this general Embodiment-Agnostic Affordance Representation, our model requires only a small amount of task-specific annotated images for fine-tuning, enabling rapid cross-platform deployment. This design ensures that the model remains object-centric, focusing solely on predicting the contact point position and trajectories of the objects that need to be manipulated, while maintaining computational efficiency and embodiment-agnostic flexibility. For different data sources, we employ distinct strategies to extract and annotate the Embodiment-Agnostic Affordance Representation.

**Dataset:** The dataset comprises four components: PixMo-One-Point, HOI4D-22k, DROID-2k, and Maniskill-5k. PixMo-One-Point includes one million single-contact-

point annotations from PixMo-Points [12]. HOI4D-22k contains 22,000 human-object interaction trajectories extracted and verified from HOI4D [33]. DROID-2k consists of 2000 verified manipulation trajectories from the DROID dataset [22], annotated using a semi-automated pipeline. Maniskill-5k includes 4965 trajectories from the ManiSkill Scene [45] dataset, converted to 2D for compatibility. For detailed descriptions of the dataset and annotation pipeline, see Appendix.

### 3.3. $A_0$ Model Structure

Figure 3 provides an overview of the proposed  $A_0$  model. Our approach builds upon the diffusion transformer architecture, DiT [38]. In our framework, a pre-trained vision encoder and a pre-trained text encoder are employed to extract features from the input image and language instruction, respectively. The resulting image and text tokens are subsequently integrated via a cross-attention mechanism, which conditions the diffusion process.

We define  $T$  waypoints as affordance representation

$$\mathbf{x}_{t:t+T}, \quad \text{where } \mathbf{x}_t = (u, v) \in [0, 1]^2 \subset \mathbb{R}^2. \quad (2)$$

$t$  denotes the  $t$ -th timestep in the trajectory.  $T$  is the future step chunk sizes.  $\mathbf{x}_t$  denotes a two-dimensional coordinate normalized according to the image size. The first point is start point, indicating the initial contact position.

The input to the  $A_0$  model comprises diffusion timestep  $k$  and noisy waypoints. Followed by DiT, the vector embedding of  $k$  is appended as additional tokens in the input

sequence. The input observation images  $I_{t-1:t}$  and language instruction  $\ell$  are incorporated as conditions via cross-attention. The observed images captured from an external camera consist of the current frame  $I_t$  and the previous frame  $I_{t-1}$ . Optionally, the previous frame can be utilized to provide motion information between the images.

We use the vision encoder of pre-trained SigLiP (400M) [59] to separately encode the observation images  $I_{t-1}, I_t$  to tokens  $I_{t-1}^1, I_{t-1}^2, \dots, I_{t-1}^{N_S}$  and  $I_t^1, I_t^2, \dots, I_t^{N_S}$ , where  $N_T$  is the number of tokens.

**Position Offset Attention.** The motion information of objects is crucial for robotic manipulation. To enable the model to pay attention on motion information, we subtract the tokens  $I_t^i$  and  $I_{t-1}^i$  to obtain  $I_m^i$ , which is then concatenated with  $I_t$  along the token dimension to serve as the final visual feature  $o_t = \text{concat}([I_t^i, I_m^i], \text{dim} = 1)$ .

Sinusoidal positional embeddings in multi-dimensional grids [31] are added to enhance the model’s ability to distinguish images based on viewpoint and time steps. We utilize pre-trained Qwen2.5-7B [54] as a robust language encoder to get tokens and masks. The image and text tokens are alternately injected in successive layers’ cross-attention blocks to compress and address the different dimensions [31]. The whole model consists of  $N$  layers of DiT blocks. Our model learns a conditional distribution  $p(\mathbf{x}_t | \ell, I_{t-1:t})$ .

**Spatial Information Aggregation Layer.** We add a final nonlinear MLP decoder as a projection from the latent space back to the physical space.

At inference stage, at timesteps  $t$ , we have language instruction  $\ell$  and images  $I_{t-1:t}$ . we sample noisy waypoints  $\mathbf{x}_{t:t+T}^k \sim \mathcal{N}(0, \mathbf{I})$ . With diffusion timesteps  $k$  and condition images and language instruction, the model can predict diffusion policies of waypoints  $\mathbf{x}_{t:t+T}$  via fast ordinary differential equation (ODE) solver [34] in  $K_D$  de-noising steps ( $K_D \ll K_F$ ). Denote  $\mathbf{x}_{t:t+T}^k$  as  $\mathbf{x}_k$ , and thus the diffusion ODE is

$$\frac{d\mathbf{x}^k}{dk} := f(k)\mathbf{x}^k + \frac{g^2(k)}{2\sigma_k} \epsilon_\theta(\mathbf{x}^k, k), \mathbf{x}^k \sim \mathcal{N}(0, \tilde{\sigma}^2 \mathbf{I}), \quad (3)$$

where  $f(k)\mathbf{x}_k$  is a linear function of  $\mathbf{x}_k$ , and  $\frac{g^2(k)}{2\sigma_k} \epsilon_\theta(\mathbf{x}_k, k)$  is generally a nonlinear function of  $x_t$  because of the neural network  $\epsilon_\theta(\mathbf{x}^k, k)$ .

### 3.4. Training Affordance Prediction Model $A_0$

**Pre-training.** The prediction of the first waypoint (start point) is crucial; subsequent waypoints can be derived by learning the offset  $\Delta x$ . The model must be capable of localizing objects based on textual descriptions. Using these images of PixMo-One-Point sourced from the Internet, we trained the  $A_0$  model to develop a general object localization capability.

To adapt to this dataset, we only use one image  $I_t$  for the vision encoder and supervise the first waypoint  $x_t^k$ , which

consists of normalized two-dimensional coordinates. The loss is MSE of ground truth and predicted coordinates:

$$\mathcal{L}_p(\theta) = \frac{1}{n} \sum_{i=1}^n ((x_t^0)_i - (f_\theta(k, x_t^k, I_t, \ell))_i)^2. \quad (4)$$

**Supervised fine-tuning.** To adapt the pre-trained  $A_0$  model to the robotic manipulation, we fine-tune the model on labeled data of specific task. In this stage, the text condition is extended from object label to language instruction. The output is extended from one point to  $T$  waypoints. The model learns dynamic robotic manipulation with motion information.

Given the ground truth waypoints  $x_{t:t+T}^0$ , for timesteps  $k \in K_F \subset \mathbb{N}^+$  of diffusion forward process, we can add noise to the ground truth and sample  $x_{t:t+T}^k = \sqrt{\bar{\alpha}^k} x_{t:t+T}^0 + \sqrt{1 - \bar{\alpha}^k} \epsilon^k$ , where  $\epsilon^k \sim \mathcal{N}(0, \mathbf{I})$ , and  $\bar{\alpha}^k$  is hyperparameter defined by the noise schedule. Given timesteps  $k$ , noisy waypoints  $x_{t:t+T}^k$  and conditions  $I_{t-1:t}$  and  $\ell$ , our model  $f_\theta$  learns to prediction the origin waypoints and minimize the mean-squared error (MSE) loss:

$$\mathcal{L}_s(\theta) = \frac{1}{n} \sum_{i=1}^n ((x_{t:t+T}^0)_i - (f_\theta(k, x_{t:t+T}^k, I_{t-1:t}, \ell))_i)^2. \quad (5)$$

## 4. Action Execution

To execute the predicted actions from our model, we transform the predicted 2D keypoints  $x_{t:t+T}$  into 3D space and determine the grasp pose using sampling based affordance lifting methods [13, 35].

### 4.1. 2D-to-3D Projection

Given the predicted 2D keypoints  $x_{t:t+T}$  from model  $A_0$ , where  $\mathbf{x}_t$  corresponds to the contact point and the remaining  $T - 1$  points represent post-contact directional cues, we employ depth-based deprojection to map them to 3D coordinates. The transformation is defined as:

$$X_i = D(\mathbf{x}_i) K^{-1} \tilde{\mathbf{x}}_i, \quad i = t + 1, t + 2, \dots, t + T, \quad (6)$$

where  $D(\mathbf{x}_i)$  is the depth value at pixel  $\mathbf{x}_i$ ,  $K$  is the camera intrinsic matrix, and  $\tilde{\mathbf{x}}_i$  represents the homogeneous coordinates of  $\mathbf{x}_i$ .

### 4.2. Grasp Pose Estimation

Following MOKA [29] and RAM [25], we refine the grasp pose by querying GraspNet [13] or other grasp samplers [35]. They generates a set of grasp candidates based on local geometric features. We select the grasp candidate  $G^*$  closest to the projected grasp point  $X_t$ :

$$G^* = \arg \min_{G \in \mathcal{G}} \|G - X_t\|, \quad (7)$$

where  $\mathcal{E}$  is the set of grasp candidates proposed by grasp samplers.

### 4.3. Waypoint Selection and Execution

For waypoint execution, we leverage the post-contact directional keypoints  $\{x_2, \dots, x_T\}$ , which are projected into 3D space using the same depth deprojection method. To determine their heights in free space, we adopt a discrete selection strategy inspired by [55]. The VLM is prompted to choose the height category (e.g., at target level or above target), and the final 3D waypoints are sampled accordingly.

The obtained grasp pose and 3D waypoints are then used to generate the motion trajectory in SE(3) space, ensuring smooth and feasible execution on the real robot.

## 5. Experiment

The primary goal of our experiments is to validate  $A_0$ 's architecture and analyze the behavior of  $A_0$  on real-world tasks with a wide range of objects and tasks. We design our experiments to investigate the following questions:

- *Is our model architecture effective for point-based affordance prediction? Does the pre-training improve performance on specific tasks?*
- *How does our approach perform in real-world scenarios? Is it platform-agnostic and transferable to other robotic systems?*
- *How does our model compare to state-of-the-art VLM-based policies and VLA policies?*

To address these questions, we design two types of experiments. First, we determine an appropriate network architecture and pretraining strategy using offline MAE evaluation metrics in Section 5.1. Then, we deploy our model on multiple robotic platforms and compare its performance with state-of-the-art methods in Section 5.2.

### 5.1. Offline Validation

we employ the Mean Absolute Error (MAE) of ground truth and predicted waypoints to evaluate the performance of our model.

$$\text{MAE} = \frac{1}{n} \sum_{i=1}^n |(\mathbf{x}_{t:t+T})_i - (\hat{\mathbf{x}}_{t:t+T})_i| \quad (8)$$

#### 5.1.1. Experimental Setting

We configure the number of transformer layers  $N=28$ , and the model contains 1 billion parameters (denoted as  $A_0$ -1B). We set the chunk size  $T=5$ , and set the number of steps for the forward and backward processes of the diffusion model,  $K_F$  and  $K_D$ , to 1000 and 5, respectively. We split the DROID-2k, HOI4D-22k, and ManiSkill-5k datasets into training and testing sets with an 8:2 ratio. 3,600 images from the PixMo-One-Point dataset are used as the test set.

During the pre-training phase, we trained the model for 200 epochs. For the supervised fine-tuning, we train the model for 40000 steps.

#### 5.1.2. Effectiveness of Pre-training

The pre-training stage of  $A_0$  is crucial for establishing foundational object localization capabilities. By training on 1 million contact-point localization samples,  $A_0$  learns to predict initial contact points based on textual instruction. We employed Real-to-Sim and Sim-to-Real paradigms, which correspond to training on HOI4D and DROID with testing on Maniskill, and training on Maniskill with testing on HOI4D and DROID, respectively.

As shown in Figure 4, pre-training can decrease the MAE of  $T$  waypoints on specific tasks. Ablation studies demonstrate that pre-training enhances  $A_0$ 's ability to generalize across unseen objects and environments. This highlights the importance of large-scale pre-training in building robust foundational capabilities for downstream robotic manipulation tasks.

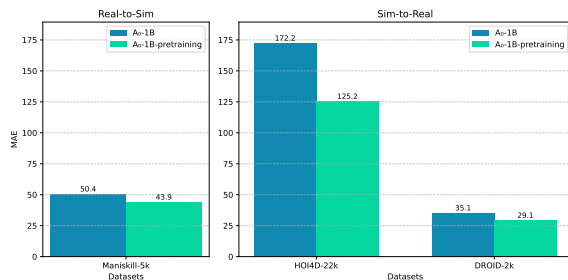


Figure 4. Performance of MAE↓ with pretraining on three datasets.

#### 5.1.3. Effectiveness of Network Structure

Table 1 show that Position Offset Attention and Spatial Information Aggregation Layer are crucial for  $A_0$ 's performance. Removing Position Offset Attention increases the MAE by 0.8 on Maniskill-5k, impairing motion-aware reasoning, especially in tasks like wiping or stacking. Without the Spatial Information Aggregation Layer, the MAE increases by 13.2 pixels on HOI4D-22k, significantly degrading waypoint prediction in complex or occluded environments.

Table 1. Ablation studies of network architecture.  $A_0$ -1B is pretrained on Pixmo-One-Point. 'POA' denotes Position Offset Attention and 'SIAL' denotes Spatial Information Aggregation Layer. We use MAE (lower is better) as evaluation metric.

MAE↓	HOI4D-22k	Maniskill-5k	DROID-2k
$A_0$ -1B	47.5	5.5	17.5
$A_0$ -1B w/o POA	47.9	6.3	18.5
$A_0$ -1B w/o SIAL	61.1	10.2	19.6

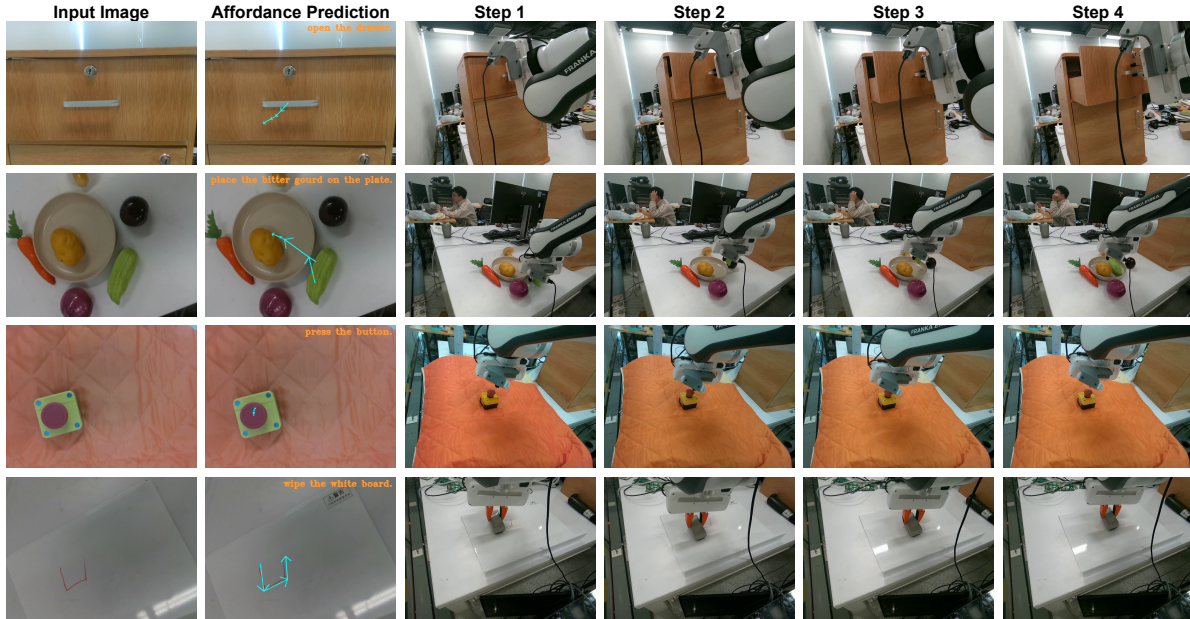


Figure 5. Evaluation on a range of complex and temporally extended tasks using the Franka Emika robot. The four tasks include opening a drawer, placing an object on a plate, pressing a button, and wiping a whiteboard. We predict 2D affordances and employ the action execution method to deploy them on the robot.

Table 2. Performance evaluation of different large language model-based policies across four manipulation tasks on two distinct robotic platforms. Our method demonstrates strong platform-agnostic capabilities by achieving consistently high success rates across both Kinova Gen3 and Franka Emika robots.

Robot	Method	Place Object	Open Drawer	Press Button	Wipe Board	Avg. Success
Kinova	MOKA	70	50	30	30	45.00
	ReKep	<b>75</b>	55	5	0	33.75
	$A_0$ -1B	60	<b>65</b>	<b>40</b>	<b>50</b>	<b>53.75</b>
Franka	Magma	25	10	30	0	16.25
	Molmo	60	40	55	20	43.75
	$A_0$ -1B	<b>60</b>	<b>75</b>	<b>70</b>	<b>45</b>	<b>62.50</b>

## 5.2. RealWorld Experiments

In this section, we evaluate  $A_0$ 's performance in real-world environments, comparing with state-of-the-art 2D affordance-based methods, MOKA[29], ReKep [20] and end-to-end approaches,  $\pi_0$  [6], RDT [31]. Our experiments were conducted on multiple robotic platforms including Franka Emika, Kinova Gen3, Realman, and Dobot X-Trainer to validate generalization capabilities across different embodiments.

### 5.2.1. Tasks Setting

For all experiments, we used a standardized environment setup with consistent object placements and camera configurations across all methods. Each robot was equipped with an RGB-D camera for visual perception. As shown in Figure 5, the testing protocol involved four common household tasks: (a) open the drawer, (b) placing an object on the plate,

(c) press the button, (d) and wipe the white board. In the following sections, these tasks are abbreviated as Place Object, Open Drawer, Press Button, and Wipe Board. For all tasks, we conducted 20 trials to calculate the success rate. Our approach takes an input image along with the corresponding instruction. After passing through  $A_0$ , it generates a 2D affordance prediction (shown in the second column of the figure). Subsequently, our action execution module transforms this prediction into an action in the SE(3) space, which is then executed by the robotic arm (shown in the right 4 columns of the figure).

### 5.2.2. Compare with 2D Affordance Methods

We compare our approach with two categories of methods: 1) MOKA [29] and ReKep [20], which utilize vision-based models to predict 2D affordances, and 2) Molmo [12] and Magma [56], which predict 2D points using Visual-

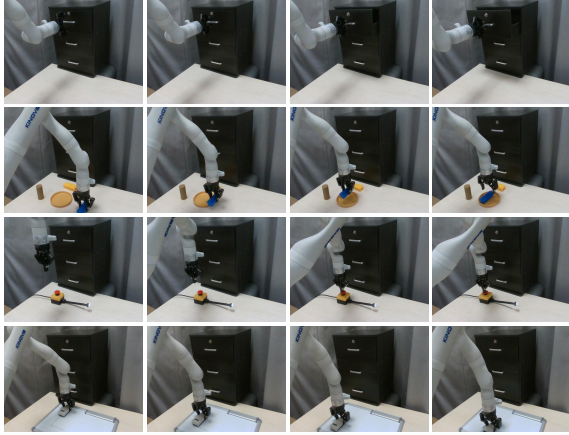


Figure 6. Qualitative evaluation of 4 tasks on Kinova. Our model performs single-shot inference, allowing for rapid execution.

Language Models (VLM) outputs and execute actions via our action execution module. The first category demonstrates the superior ability of our model in **spatial affordance understanding**, while the second category shows that **action execution module** can be seamlessly integrated into other methods, exhibiting strong generalization capabilities. We reproduced MOKA and ReKep on the Kinova platform. For Magma and Molmo, we obtained 2D points by feeding the camera input and prompts into their models, then executed the actions using our action execution module. The results are shown in Table 2. Notably, it excels in trajectory-based tasks such as Wipe Board, where precise motion execution is critical. Our approach achieves an average success rate of 62.50% on Franka, outperforming the next best method (Molmo: 43.75%) by 18.75 percentage points. On Kinova, our method achieves 53.75%, showing a 20 percentage point improvement over the weakest baseline (ReKep: 33.75%). Particularly in the Open Drawer task, our model achieves 75%, surpassing all competitors, and in the Wipe Board task, it reaches 45%, demonstrating significant robustness in trajectory tracking. Our method performs slightly weaker than MOKA and ReKep on the Place Object task on the Kinova. A possible reason for this is that these methods, based on vision foundation models like SAM [24] and GPT-4 [1], have encountered a vast number of real-world physical objects during their training. We also compare with Robopoint. Details are in supporting materials.

### 5.2.3. Compare with Vision-Language-Action Methods

We also conducted a comparative analysis with the latest End-to-End Vision-Language-Action (VLA) large model, specifically RDT-1B [31] and  $\pi_0$  [6]. RDT-1B is a 1-billion-parameter Diffusion Transformer for imitation learning, pre-trained on over 1 million multi-robot episodes. RDT unifies the actions of different robots into a 128-

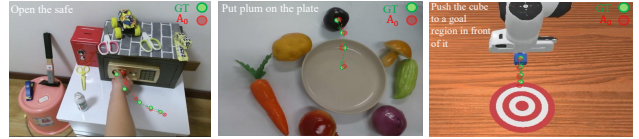


Figure 7.  $A_0$  can predict accurately on different datasets. These three images are sourced from Droid, our Franka robot, and the ManiSkill simulation environment.

dimensional space while supporting flexible input and output configurations.  $\pi_0$  proposes a novel flow matching architecture built on top of a pre-trained VLM to inherit Internet-scale semantic knowledge. To demonstrate the superiority of our method on trajectory-based tasks, we collected 5 episodes image-action data for the Wipe Board task, which includes third-view images and wrist images. We fine-tuned these two models and conducted experiments on the single-arm Kinova robot. The experimental results, as shown in Table 3, indicate that our method outperforms the second-best method by 15%. Additionally, since our model requires only a single inference and does not rely on the iterative outputs of VLA methods, the execution speed of our tasks is significantly faster, with execution steps being 1/8 to 1/10 of those required by VLA methods.

Table 3. Comparison with RDT-1B and  $\pi_0$  on the Wipe Board task using the Kinova platform, highlighting our method’s superiority in trajectory-following and task execution efficiency.

	Wipe Board	Steps
RDT-1B [31]	10	25-50
$\pi_0$ [6]	35	25-50
$\pi_0$ + FAST [6]	30	25-50
$A_0$ -1B	<b>50</b>	<b>4-5</b>

### 5.2.4. Qualitative Evaluation

In Figures 5 and 6, we present 8 examples of our method. The method in Figure 5 is performed on the Franka platform, while the method in Figure 6 is executed on the Kinova platform. The image sequences of task execution in these 8 examples effectively demonstrate that our method is platform-agnostic. Since our method is based on single-shot inference, the robot can be deployed and execute tasks very quickly. We also demonstrate the performance of  $A_0$  across diverse datasets in Figure 7.

## 6. Conclusion

In this paper, we present  $A_0$ , a hierarchical affordance-aware diffusion model for robotic manipulation. By decomposing tasks into high-level spatial affordance reasoning and low-level action execution,  $A_0$  uses an Embodiment-Agnostic Affordance Representation to predict object-



centric contact points and trajectories, enabling generalization across robotic platforms. Pre-trained on 1 million contact points and fine-tuned on annotated trajectories,  $A_0$  outperforms state-of-the-art methods in tasks like wiping and stacking. Key components like Position Offset Attention and Spatial Information Aggregation enhance spatial reasoning and efficiency. Experiments on Franka, Kinova, Realman, and Dobot validate  $A_0$ 's robustness and real-world applicability. Future work will extend  $A_0$  to dynamic and unstructured environments.

# A<sub>0</sub>: An Affordance-Aware Hierarchical Model for General Robotic Manipulation

## Supplementary Material

### A. Social Impact

The internet datasets we used, PixMo-Points, HOI4D, and the real-robot dataset Droid, are all publicly available and transparent. The ManiSkill-5k dataset was collected in a simulation environment, while the real-robot datasets we collected do not contain any personal information. We plan to release these datasets in the future. Our method has no ethical risk on dataset usage and privacy violation since all the benchmarks are publicly available and transparent.

### B. Limitations and Future work

#### B.1. Limitations

Our method has two main limitations:

- Our model relies on methods like gripper samplers to predict grasp poses for action execution. However, existing approaches in this area often exhibit suboptimal performance and limited generalization across different tasks.
- Our method requires a depth map to estimate height, followed by refinement using a VLM. However, this approach may not perform well in tasks involving occluded objects.

#### B.2. Future Work

Based on our analysis of the limitations of our method, we plan to pursue the following future work:

- First, improving grasp pose estimation: Our current method relies on a gripper sampler to obtain grasp poses. A potential improvement could be leveraging a VLM to visually assist in selecting the best gripper position from gripper candidates or directly prompting the VLM to generate a grasp pose.
- Second, improving height estimation: Currently, the grasp height is obtained by prompting an LLM. We can refine our model by incorporating depth, gripper length, and other relevant information as conditions to directly predict the height.

### C. Dataset

We have collected data from four types of sources: internet data, real-robot data, human-centric data, and simulator data. Below is a detailed description of each of these four types of data.

**Contact-point Localization Data:** We select one million samples with only a single coordinate point (contact point  $c_0^{2D}$ ) annotation from the PixMo-Points [12] dataset, named PixMo-One-Point. Every sample consists of one image, object label and corresponding coordinate.

**Real Robotic Data:** We developed a multi-stage annotation pipeline to capture high-quality manipulation trajectories from real robotic interactions. Human annotators identified target objects and initial contact points in videos, followed by automatic tracking using the CoTracker model [21] to generate trajectory waypoints. In the second method, we employed Molmo [12] to annotate the initial point and subsequently used SAM2 [42] to segment and track the object mask across frames. Each trajectory was manually verified for accuracy. This semi-automated approach produced a dataset of verified manipulation waypoints. We randomly selected and annotated 2,000 trajectory samples from the DROID [22] dataset, naming it DROID-2k.

**Human-centric Data:** Compared to robot interaction data, video-based human-object interaction data like HOI4D [33] are more accessible and semantically rich. The HOI4D dataset [33] encompasses 16 distinct object categories (e.g., toy cars, bottles) and covers 6 different tasks, including pick-and-place, opening a drawer, and pulling a toy car. Each category includes multiple videos, amounting to a total of 3,572 videos. Each video is comprised of several segmented actions, and by employing various action labels to delineate these segments, a total of 22,140 unique video segments were obtained. We convert the original dataset into a 2D waypoint format, where the center point of the object’s 2D mask in each frame is used as the waypoint, and the combination of the action and object name serves as the instruction. We refer to the transformed dataset as HOI4D-22k.

**Simulator Data:** To adapt our model for various deployment environments, we collected 4965 trajectories from the ManiSkill Scene dataset, converting 3D data to 2D for compatibility. There are five tasks: “Peg Insertion Side”, “Plug Charger”, “Pull Cube Tool”, “Push Cube”, and “Stack Cube”. Each task contains about a thousand trajectories. We named this dataset Maniskill-5k. Camera angles were adjusted to diversify scene data.

The image resolutions of the HOI4D, Maniskill, and DROID datasets are 1920×1080, 512×512, and 320×180, respectively.

### D. Compare with Robopoint

To compare our approach with Robopoint, we evaluated both methods on two standard datasets: HOI4D and DROID. We measured the Mean Absolute Error (MAE) of the first predicted interaction pixel compared to the ground truth. For our model, we used the first waypoint directly,

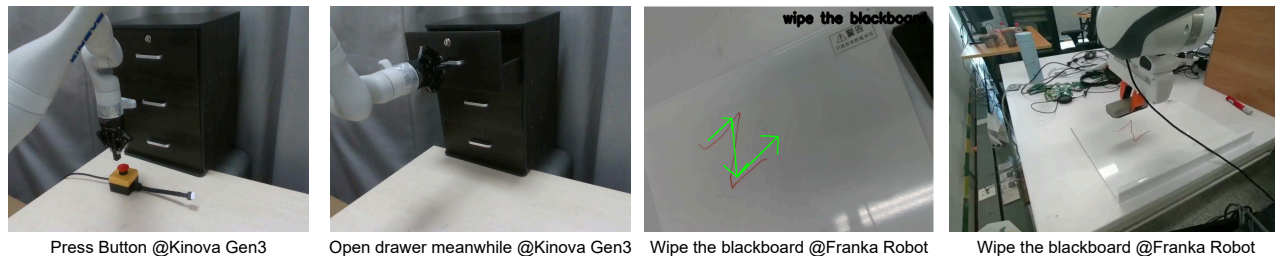


Figure 8. Real World Kinova Gen3 Robot

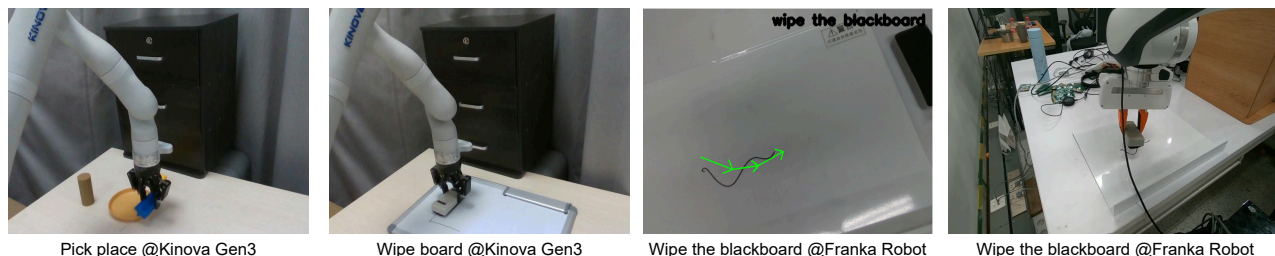


Figure 9. Real World Franka Robot

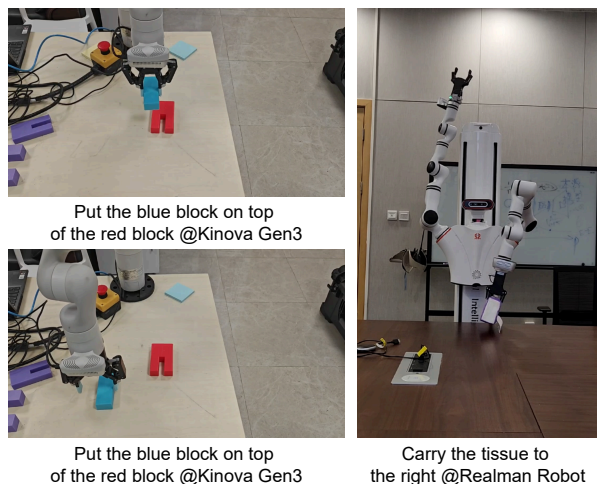


Figure 10. Real World Kinova Gen3 Robot and Realman Robot

while for Robopoint, which predicts interaction regions rather than specific points, we used the average position of all predicted points for comparison.

As shown in Table 3, our method achieves substantially lower MAE scores across both datasets. Specifically, on HOI4D, our model achieves an MAE of 54.46 compared to Robopoint’s 121.09, representing a 55.2% reduction in error. Similarly, on DROID, our approach attains an MAE of 14.13 versus Robopoint’s 27.47, a 40.4% improvement. These results demonstrate that our method provides more precise interaction point predictions, which is crucial for ac-

curate robot manipulation tasks.

Method	HOI4D (MAE)	DROID (MAE)
Robopoint	121.09	27.47
Ours	<b>54.46</b>	<b>14.13</b>

Table 4. Comparison of Mean Absolute Error (MAE) for the first interaction pixel between our method and Robopoint on HOI4D and DROID datasets. Lower values indicate better performance.

## E. Real World Experiment

We conduct our real world robot experiments on multiple robot platforms, including Kinova, Franka, and Realman Robot, as shown in Figure 8, Figure 9 and Figure 10.

## F. Annotation platform

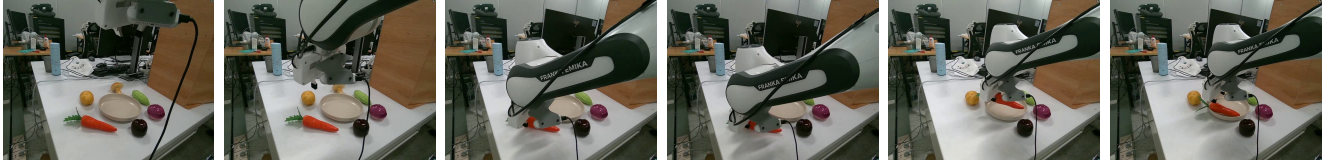
Our annotation platform is a multi-source, semi-automated system designed to generate high-quality spatial affordance data for robotic manipulation. It integrates real robotic interactions, human-object interaction datasets, simulation environments, and large-scale internet-sourced datasets to create a standardized Embodiment-Agnostic Affordance Representation.

## G. Additional Qualitative Result on Franka

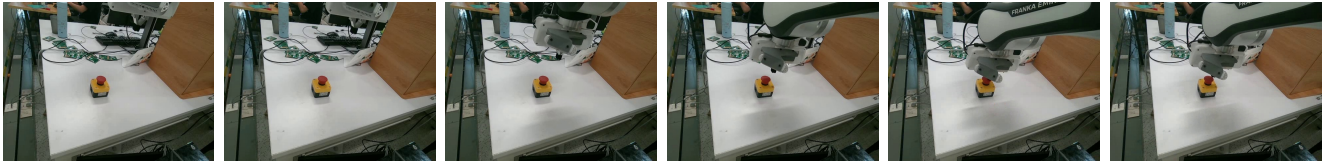
As shown in Fig. 11, our approach generalizes well to different backgrounds on Franka Robot. The text below each raw of images serves as the instruction.



Put the bitter guard on the plate.



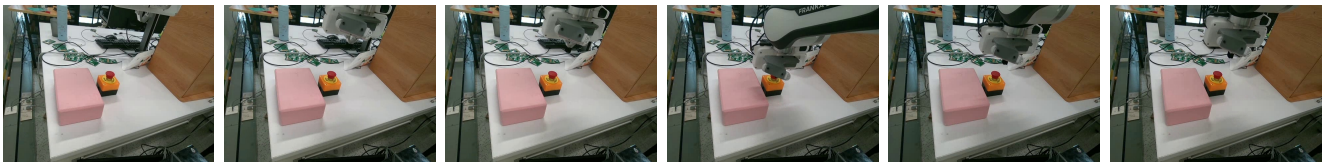
Put the wild carrot on the plate.



Press the button.



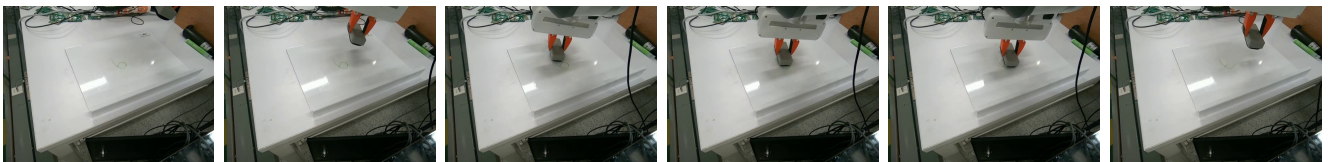
Press the button.



Press the button.



Wipe the white board.



Wipe the white board.

Figure 11. Real World Franka Robot.

## References

- [1] Gpt-4v(ision) system card. 2023. 8
- [2] Anas Awadalla, Irena Gao, Josh Gardner, Jack

Hessel, Yusuf Hanafy, Wanrong Zhu, Kalyani Marathe, Yonatan Bitton, Samir Gadre, Shiori Sagawa, Jenia Jitsev, Simon Kornblith, Pang Wei Koh, Gabriel Ilharco, Mitchell Wortsman, and Lud-

- wig Schmidt. OpenFlamingo: An Open-Source Framework for Training Large Autoregressive Vision-Language Models, 2023. 3
- [3] Shikhar Bahl, Russell Mendonca, Lili Chen, Unnat Jain, and Deepak Pathak. Affordances from Human Videos as a Versatile Representation for Robotics, 2023. 3
- [4] Homanga Bharadhwaj, Debidatta Dwibedi, Abhinav Gupta, Shubham Tulsiani, Carl Doersch, Ted Xiao, Dhruv Shah, Fei Xia, Dorsa Sadigh, and Sean Kirmani. Gen2Act: Human Video Generation in Novel Scenarios enables Generalizable Robot Manipulation, 2024. 3
- [5] Homanga Bharadhwaj, Roozbeh Mottaghi, Abhinav Gupta, and Shubham Tulsiani. Track2act: Predicting point tracks from internet videos enables generalizable robot manipulation. In *European Conference on Computer Vision*, pages 306–324. Springer, 2024. 2
- [6] Kevin Black, Noah Brown, Danny Driess, Adnan Esmail, Michael Equi, Chelsea Finn, Niccolo Fusai, Lachy Groom, Karol Hausman, Brian Ichter, et al.  $\pi_0$ : A vision-language-action flow model for general robot control. *arXiv preprint arXiv:2410.24164*, 2024. 1, 7, 8
- [7] Anthony Brohan, Noah Brown, Justice Carbajal, Yevgen Chebotar, Xi Chen, Krzysztof Choromanski, Tianli Ding, Danny Driess, Avinava Dubey, Chelsea Finn, Pete Florence, Chuyuan Fu, Montse Gonzalez Arenas, Keerthana Gopalakrishnan, Kehang Han, Karol Hausman, Alexander Herzog, Jasmine Hsu, Brian Ichter, Alex Irpan, Nikhil Joshi, Ryan Julian, Dmitry Kalashnikov, Yuheng Kuang, Isabel Leal, Lisa Lee, Tsang-Wei Edward Lee, Sergey Levine, Yao Lu, Henryk Michalewski, Igor Mordatch, Karl Pertsch, Kanishka Rao, Krista Reymann, Michael Ryoo, Grecia Salazar, Pannag Sanketi, Pierre Sermanet, Jaspier Singh, Anikait Singh, Radu Soricut, Huong Tran, Vincent Vanhoucke, Quan Vuong, Ayzaan Wahid, Stefan Welker, Paul Wohlhart, Jialin Wu, Fei Xia, Ted Xiao, Peng Xu, Sichun Xu, Tianhe Yu, and Brianna Zitkovich. Rt-2: Vision-language-action models transfer web knowledge to robotic control, 2023. 1
- [8] Anthony Brohan, Noah Brown, Justice Carbajal, Yevgen Chebotar, Xi Chen, Krzysztof Choromanski, Tianli Ding, Danny Driess, Avinava Dubey, Chelsea Finn, Pete Florence, Chuyuan Fu, Montse Gonzalez Arenas, Keerthana Gopalakrishnan, Kehang Han, Karol Hausman, Alexander Herzog, Jasmine Hsu, Brian Ichter, Alex Irpan, Nikhil Joshi, Ryan Julian, Dmitry Kalashnikov, Yuheng Kuang, Isabel Leal, Lisa Lee, Tsang-Wei Edward Lee, Sergey Levine, Yao Lu, Henryk Michalewski, Igor Mordatch, Karl Pertsch, Kanishka Rao, Krista Reymann, Michael Ryoo, Grecia Salazar, Pannag Sanketi, Pierre Sermanet, Jaspier Singh, Anikait Singh, Radu Soricut, Huong Tran, Vincent Vanhoucke, Quan Vuong, Ayzaan Wahid, Stefan Welker, Paul Wohlhart, Jialin Wu, Fei Xia, Ted Xiao, Peng Xu, Sichun Xu, Tianhe Yu, and Brianna Zitkovich. RT-2: Vision-Language-Action Models Transfer Web Knowledge to Robotic Control, 2023. 3
- [9] Chi-Lam Cheang, Guangzeng Chen, Ya Jing, Tao Kong, Hang Li, Yifeng Li, Yuxiao Liu, Hongtao Wu, Jiafeng Xu, Yichu Yang, Hanbo Zhang, and Minzhao Zhu. GR-2: A Generative Video-Language-Action Model with Web-Scale Knowledge for Robot Manipulation, 2024. 3
- [10] Joya Chen, Difei Gao, Kevin Qinghong Lin, and Mike Zheng Shou. Affordance Grounding from Demonstration Video to Target Image, 2023. 3
- [11] Xi Chen, Josip Djolonga, Piotr Padlewski, Basil Mustafa, Soravit Changpinyo, Jialin Wu, Carlos Riquelme Ruiz, Sebastian Goodman, Xiao Wang, Yi Tay, Siamak Shakeri, Mostafa Dehghani, Daniel Salz, Mario Lucic, Michael Tschannen, Arsha Nagrani, Hexiang Hu, Mandar Joshi, Bo Pang, Ceslee Montgomery, Paulina Pietrzyk, Marvin Ritter, A. J. Piergiovanni, Matthias Minderer, Filip Pavetic, Austin Waters, Gang Li, Ibrahim Alabdulmohsin, Lucas Beyer, Julien Amelot, Kenton Lee, Andreas Peter Steiner, Yang Li, Daniel Keysers, Anurag Arnab, Yuanzhong Xu, Keran Rong, Alexander Kolesnikov, Mojtaba Seyedhosseini, Anelia Angelova, Xiaohua Zhai, Neil Houlsby, and Radu Soricut. PaLI-X: On Scaling up a Multilingual Vision and Language Model, 2023. 3
- [12] Matt Deitke, Christopher Clark, Sangho Lee, Rohun Tripathi, Yue Yang, Jae Sung Park, Mohammadreza Salehi, Niklas Muennighoff, Kyle Lo, Luca Soldaini, et al. Molmo and pixmo: Open weights and open data for state-of-the-art multimodal models. *arXiv preprint arXiv:2409.17146*, 2024. 1, 4, 7, 10
- [13] Hao-Shu Fang, Chenxi Wang, Minghao Gou, and Cewu Lu. Graspnet-1billion: A large-scale benchmark for general object grasping. In *Proceedings of the IEEE/CVF conference on computer vision and pattern recognition*, pages 11444–11453, 2020. 5
- [14] Figure AI Team. Helix: Our first humanoid robot, 2025. Accessed: 2025-03-07. 3
- [15] Yiran Geng, Boshi An, Haoran Geng, Yuanpei Chen, Yaodong Yang, and Hao Dong. End-to-End Affordance Learning for Robotic Manipulation, 2022. 3
- [16] Zhi Hou, Tianyi Zhang, Yuwen Xiong, Hengjun Pu, Chengyang Zhao, Ronglei Tong, Yu Qiao, Jifeng Dai, and Yuntao Chen. Diffusion Transformer Policy:

- Scaling Diffusion Transformer for Generalist Vision-Language-Action Learning, 2025. 3
- [17] Siyuan Huang, Haonan Chang, Yuhan Liu, Yimeng Zhu, Hao Dong, Peng Gao, Abdeslam Boularias, and Hongsheng Li. A3VLM: Actionable Articulation-Aware Vision Language Model, 2024. 3
- [18] Siyuan Huang, Iaroslav Ponomarenko, Zhengkai Jiang, Xiaoqi Li, Xiaobin Hu, Peng Gao, Hongsheng Li, and Hao Dong. ManipVQA: Injecting Robotic Affordance and Physically Grounded Information into Multi-Modal Large Language Models, 2024. 3
- [19] Wenlong Huang, Chen Wang, Yunzhu Li, Ruohan Zhang, and Li Fei-Fei. ReKep: Spatio-Temporal Reasoning of Relational Keypoint Constraints for Robotic Manipulation. 3
- [20] Wenlong Huang, Chen Wang, Yunzhu Li, Ruohan Zhang, and Li Fei-Fei. Rekep: Spatio-temporal reasoning of relational keypoint constraints for robotic manipulation. *arXiv preprint arXiv:2409.01652*, 2024. 1, 7
- [21] Nikita Karaev, Ignacio Rocco, Benjamin Graham, Natalia Neverova, Andrea Vedaldi, and Christian Rupprecht. Cotracker: It is better to track together. *arXiv:2307.07635*, 2023. 10
- [22] Alexander Khazatsky, Karl Pertsch, Suraj Nair, Ashwin Balakrishna, Sudeep Dasari, Siddharth Karamcheti, Soroush Nasiriany, Mohan Kumar Srirama, Lawrence Yunliang Chen, Kirsty Ellis, et al. Droid: A large-scale in-the-wild robot manipulation dataset. *arXiv preprint arXiv:2403.12945*, 2024. 4, 10
- [23] Moo Jin Kim, Karl Pertsch, Siddharth Karamcheti, Ted Xiao, Ashwin Balakrishna, Suraj Nair, Rafael Rafailov, Ethan P Foster, Pannag R Sanketi, Quan Vuong, et al. Openvla: An open-source vision-language-action model. In *8th Annual Conference on Robot Learning*. 1, 3
- [24] Alexander Kirillov, Eric Mintun, Nikhila Ravi, Hanzi Mao, Chloe Rolland, Laura Gustafson, Tete Xiao, Spencer Whitehead, Alexander C. Berg, Wan-Yen Lo, Piotr Dollár, and Ross Girshick. Segment anything. *arXiv:2304.02643*, 2023. 8
- [25] Yuxuan Kuang, Junjie Ye, Haoran Geng, Jiageng Mao, Congyue Deng, Leonidas Guibas, He Wang, and Yue Wang. Ram: Retrieval-based affordance transfer for generalizable zero-shot robotic manipulation. *arXiv preprint arXiv:2407.04689*, 2024. 1, 3, 5
- [26] Qixiu Li, Yaobo Liang, Zeyu Wang, Lin Luo, Xi Chen, Mozheng Liao, Fangyun Wei, Yu Deng, Sicheng Xu, Yizhong Zhang, Xiaofan Wang, Bei Liu, Jianlong Fu, Jianmin Bao, Dong Chen, Yuanchun Shi, Jiaolong Yang, and Baining Guo. CogACT: A Foundational Vision-Language-Action Model for Synergizing Cognition and Action in Robotic Manipulation, 2024. 3
- [27] Yicong Li, Na Zhao, Junbin Xiao, Chun Feng, Xiang Wang, and Tat-seng Chua. LASO: Language-Guided Affordance Segmentation on 3D Object. In *2024 IEEE/CVF Conference on Computer Vision and Pattern Recognition (CVPR)*, pages 14251–14260, 2024. 3
- [28] Suhan Ling, Yian Wang, Shiguang Wu, Yuzheng Zhuang, Tianyi Xu, Yu Li, Chang Liu, and Hao Dong. Articulated Object Manipulation with Coarse-to-fine Affordance for Mitigating the Effect of Point Cloud Noise, 2024. 3
- [29] Fangchen Liu, Kuan Fang, Pieter Abbeel, and Sergey Levine. Moka: Open-vocabulary robotic manipulation through mark-based visual prompting. In *First Workshop on Vision-Language Models for Navigation and Manipulation at ICRA 2024*, 2024. 1, 3, 5, 7
- [30] Fangchen Liu, Kuan Fang, Pieter Abbeel, and Sergey Levine. MOKA: Open-World Robotic Manipulation through Mark-Based Visual Prompting, 2024. 3
- [31] Songming Liu, Lingxuan Wu, Bangguo Li, Hengkai Tan, Huayu Chen, Zhengyi Wang, Ke Xu, Hang Su, and Jun Zhu. Rdt-1b: a diffusion foundation model for bimanual manipulation. *arXiv preprint arXiv:2410.07864*, 2024. 1, 5, 7, 8
- [32] Songming Liu, Lingxuan Wu, Bangguo Li, Hengkai Tan, Huayu Chen, Zhengyi Wang, Ke Xu, Hang Su, and Jun Zhu. RDT-1B: A Diffusion Foundation Model for Bimanual Manipulation, 2024. 3
- [33] Yunze Liu, Yun Liu, Che Jiang, Kangbo Lyu, Weikang Wan, Hao Shen, Boqiang Liang, Zhoujie Fu, He Wang, and Li Yi. Hoi4d: A 4d egocentric dataset for category-level human-object interaction. In *Proceedings of the IEEE/CVF Conference on Computer Vision and Pattern Recognition*, pages 21013–21022, 2022. 4, 10
- [34] Cheng Lu, Yuhao Zhou, Fan Bao, Jianfei Chen, Chongxuan Li, and Jun Zhu. Dpm-solver: A fast ode solver for diffusion probabilistic model sampling in around 10 steps. *Advances in Neural Information Processing Systems*, 35:5775–5787, 2022. 5
- [35] Lucas Manuelli, Wei Gao, Peter R. Florence, and Russ Tedrake. kpm: Keypoint affordances for category-level robotic manipulation. *CoRR*, abs/1903.06684, 2019. 5
- [36] Kaichun Mo, Leonidas Guibas, Mustafa Mukadam, Abhinav Gupta, and Shubham Tulsiani. Where2Act: From Pixels to Actions for Articulated 3D Objects, 2021. 3
- [37] Tim Pearce, Tabish Rashid, Anssi Kanervisto, Dave Bignell, Mingfei Sun, Raluca Georgescu, Sergio Valcarcel Macua, Shan Zheng Tan, Ida Momennejad, Katja Hofmann, and Sam Devlin. Imitating human behaviour with diffusion models, 2023. 3

- [38] William Peebles and Saining Xie. Scalable diffusion models with transformers. In *Proceedings of the IEEE/CVF international conference on computer vision*, pages 4195–4205, 2023. 4
- [39] Shengyi Qian, Weifeng Chen, Min Bai, Xiong Zhou, Zhuowen Tu, and Li Erran Li. AffordanceLLM: Grounding Affordance from Vision Language Models, 2024. 3
- [40] Delin Qu, Haoming Song, Qizhi Chen, Yuanqi Yao, Xinyi Ye, Yan Ding, Zhigang Wang, JiaYuan Gu, Bin Zhao, Dong Wang, and Xuelong Li. SpatialVLA: Exploring Spatial Representations for Visual-Language-Action Model, 2025. 3
- [41] Delin Qu, Haoming Song, Qizhi Chen, Yuanqi Yao, Xinyi Ye, Yan Ding, Zhigang Wang, JiaYuan Gu, Bin Zhao, Dong Wang, et al. Spatialvla: Exploring spatial representations for visual-language-action model. *arXiv preprint arXiv:2501.15830*, 2025. 2
- [42] Nikhila Ravi, Valentin Gabeur, Yuan-Ting Hu, Ronghang Hu, Chaitanya Ryali, Tengyu Ma, Haitham Khedr, Roman Rädle, Chloe Rolland, Laura Gustafson, et al. Sam 2: Segment anything in images and videos. *arXiv preprint arXiv:2408.00714*, 2024. 10
- [43] Moritz Reuss, Maximilian Li, Xiaogang Jia, and Rudolf Lioutikov. Goal-conditioned imitation learning using score-based diffusion policies, 2023. 3
- [44] Stone Tao, Fanbo Xiang, Arth Shukla, Yuzhe Qin, Xander Hinrichsen, Xiaodi Yuan, Chen Bao, Xinsong Lin, Yulin Liu, Tse-kai Chan, et al. Maniskill3: Gpu parallelized robotics simulation and rendering for generalizable embodied ai. *arXiv preprint arXiv:2410.00425*, 2024. 1
- [45] Stone Tao, Fanbo Xiang, Arth Shukla, Yuzhe Qin, Xander Hinrichsen, Xiaodi Yuan, Chen Bao, Xinsong Lin, Yulin Liu, Tse kai Chan, Yuan Gao, Xuanlin Li, Tongzhou Mu, Nan Xiao, Arnav Gurha, Zhiao Huang, Roberto Calandra, Rui Chen, Shan Luo, and Hao Su. Maniskill3: Gpu parallelized robotics simulation and rendering for generalizable embodied ai. *arXiv preprint arXiv:2410.00425*, 2024. 4
- [46] Octo Model Team, Dibya Ghosh, Homer Walke, Karl Pertsch, Kevin Black, Oier Mees, Sudeep Dasari, Joey Hejna, Tobias Kreiman, Charles Xu, Jianlan Luo, You Liang Tan, Lawrence Yunliang Chen, Panag Sanketi, Quan Vuong, Ted Xiao, Dorsa Sadigh, Chelsea Finn, and Sergey Levine. Octo: An Open-Source Generalist Robot Policy, 2024. 3
- [47] Ruicheng Wang, Jialiang Zhang, Jiayi Chen, Yinzhen Xu, Puhao Li, Tengyu Liu, and He Wang. Dexgraspnet: A large-scale robotic dexterous grasp dataset for general objects based on simulation, 2022. 3
- [48] Yian Wang, Ruihai Wu, Kaichun Mo, Jiaqi Ke, Qingnan Fan, Leonidas Guibas, and Hao Dong. AdaAfford: Learning to Adapt Manipulation Affordance for 3D Articulated Objects via Few-shot Interactions, 2023. 3
- [49] Chuan Wen, Xingyu Lin, John So, Kai Chen, Qi Dou, Yang Gao, and Pieter Abbeel. Any-point trajectory modeling for policy learning. *arXiv preprint arXiv:2401.00025*, 2023. 2
- [50] Youpeng Wen, Junfan Lin, Yi Zhu, Jianhua Han, Hang Xu, Shen Zhao, and Xiaodan Liang. Vidman: Exploiting implicit dynamics from video diffusion model for effective robot manipulation, 2024. 3
- [51] Hongtao Wu, Ya Jing, Chilam Cheang, Guangzeng Chen, Jiafeng Xu, Xinghang Li, Minghuan Liu, Hang Li, and Tao Kong. Unleashing Large-Scale Video Generative Pre-training for Visual Robot Manipulation, 2023. 3
- [52] Ruihai Wu, Yan Zhao, Kaichun Mo, Zizheng Guo, Yian Wang, Tianhao Wu, Qingnan Fan, Xuelin Chen, Leonidas Guibas, and Hao Dong. VAT-Mart: Learning Visual Action Trajectory Proposals for Manipulating 3D ARTiculated Objects, 2022. 3
- [53] Mengda Xu, Zhenjia Xu, Yinghao Xu, Cheng Chi, Gordon Wetzstein, Manuela Veloso, and Shuran Song. Flow as the cross-domain manipulation interface. In *8th Annual Conference on Robot Learning*. 2
- [54] An Yang, Baosong Yang, Beichen Zhang, Binyuan Hui, Bo Zheng, Bowen Yu, Chengyuan Li, Dayiheng Liu, Fei Huang, Haoran Wei, et al. Qwen2. 5 technical report. *arXiv preprint arXiv:2412.15115*, 2024. 4, 5
- [55] Jianwei Yang, Hao Zhang, Feng Li, Xueyan Zou, Chunyuan Li, and Jianfeng Gao. Set-of-mark prompting unleashes extraordinary visual grounding in gpt-4v, 2023. 6
- [56] Jianwei Yang, Reuben Tan, Qianhui Wu, Ruijie Zheng, Baolin Peng, Yongyuan Liang, Yu Gu, Mu Cai, Seonghyeon Ye, Joel Jang, et al. Magma: A foundation model for multimodal ai agents. *arXiv preprint arXiv:2502.13130*, 2025. 7
- [57] Chengbo Yuan, Chuan Wen, Tong Zhang, and Yang Gao. General flow as foundation affordance for scalable robot learning. In *8th Annual Conference on Robot Learning*, . 1, 2
- [58] Wentao Yuan, Jiafei Duan, Valts Blukis, Wilbert Pumacay, Ranjay Krishna, Adithyavairavan Murali, Arsalan Mousavian, and Dieter Fox. Robopoint: A vision-language model for spatial affordance prediction in robotics. In *8th Annual Conference on Robot Learning*, . 2
- [59] Xiaohua Zhai, Basil Mustafa, Alexander Kolesnikov, and Lucas Beyer. Sigmoid loss for language image

pre-training. In *Proceedings of the IEEE/CVF international conference on computer vision*, pages 11975–11986, 2023. [4](#), [5](#)

- [60] Haoyu Zhen, Xiaowen Qiu, Peihao Chen, Jincheng Yang, Xin Yan, Yilun Du, Yining Hong, and Chuang Gan. 3D-VLA: A 3D Vision-Language-Action Generative World Model, 2024. [3](#)
- [61] Yi Li, Yuquan Deng, Jesse Zhang, Joel Jang, Marius Memmel, Raymond Yu, Caelan Reed Garrett, Fabio Ramos, Dieter Fox, Anqi Li, Abhishek Gupta, Ankit Goyal. HAMSTER: Hierarchical action models for open-world robot manipulation, 2025 [3](#)